

## A THEORETICAL STUDY OF UNSATURATED OLEFIN HYDROGENATION AND ISOMERIZATION ON Pd(111)

PATRICIA G. BELELLI<sup>\*,†</sup> and NORBERTO J. CASTELLANI<sup>\*,‡</sup>

*\*Grupo de Materiales y Sistemas Catalíticos,  
Departamento de Física (UNS), Avenida Alem 1253,  
Bahía Blanca B8000CPB, Argentina*

*<sup>†</sup>pbelelli@plapiqui.edu.ar*

*<sup>‡</sup>castella@criba.edu.ar*

Received 3 September 2007

The addition of hydrogen to the carbon–carbon double bond of 2-butenes adsorbed on Pd(111) was studied within the density functional theory (DFT) and using a periodic slab model. For that purpose, the Horiuti–Polanyi mechanisms for both complete hydrogenation and isomerization were considered. The hydrogenation of *cis* and *trans*-2-butene to produce butane proceeds via the formation of *eclipsed* and *staggered*-2-butyl intermediates, respectively. In both cases, a relatively high energy barrier to produce the half-hydrogenated intermediate makes the first hydrogen addition the slowest step of the reaction. The competitive production of *trans*-2-butene from *cis*-2-butene requires the conversion from the *eclipsed*-2-butyl to the *staggered*-2-butyl isomer. As the corresponding energy barrier is relatively small and because the first of these isomers is less stable than the second, an easy conversion is predicted.

*Keywords:* Olefin adsorption and reaction; Pd(111) surface; DFT calculations.

### 1. Introduction

The catalytic hydrogenation of unsaturated organic compounds is a very important process with numerous industrial applications.<sup>1</sup> For example, the selective opening of carbon–carbon double bonds and their saturation with hydrogen atoms from a gaseous H<sub>2</sub> source is the dominant process in the synthesis of fine and specialty chemicals.<sup>2</sup> The same role has in the synthesis of food additives.<sup>3</sup> The selective hydrogenation of steam-cracking cuts constitutes a very important petrochemical process, which is used to eliminate most of the alkynes, dienes, and other troublesome compounds in olefinic streams.<sup>4</sup>

Early works in this field proposed several mechanisms for the addition of hydrogen to olefins.<sup>5</sup> The Horiuti–Polanyi mechanism considers the formation of an alkyl intermediate from coadsorbed olefin and atomic hydrogen to yield the corresponding alkane. The mechanistic studies of olefin hydrogenation profited from modern H–D exchange, temperature-programmed desorption, and high-resolution infrared spectroscopy experiments performed for ethylene and propylene adsorbed on Pt.<sup>6,7</sup> They showed that under vacuum conditions a stepwise hydrogenation is present and that an initial half-hydrogenated species (likely an alkyl) is produced. During the hydrogenation, olefins can be converted

---

<sup>‡</sup>Corresponding author.

by competing isomerization processes where also an alkyl intermediate is likely to be involved.<sup>8</sup> This kind of processes is of high relevance in the edible oil industry because the conversion from *cis* to *trans* geometrical isomer in a fatty acid is an unwanted process for the human health.<sup>9</sup> Recent high-vacuum studies have been performed for C<sub>4</sub> olefins on Pt to elucidate the mechanism of double-bond isomerization.<sup>10,11</sup>

Transition metals of the same column, like platinum and palladium, show different catalytic behavior. For example, the hydrogenation of the 1,3-butadiene on palladium catalyst is highly selective for the partially hydrogenate product (mainly 1-butene) while platinum catalyst is less active and also less selective.<sup>12,13</sup> Experiments for 1-butene and *cis*-2-butene hydrogenation/isomerization reactions show that the hydrogenation rate is insensitive to the surface structures for Pt catalysts while the isomerization rate changes significantly on stepped platinum surfaces.<sup>14</sup>

A few recent investigations have been published where the adsorption energies of different unsaturated C<sub>4</sub> hydrocarbons on Pt(111) and Pd(111) surfaces were theoretically evaluated.<sup>15</sup> One conclusion was that the lower stability of the 1-butene on Pd versus Pt may be a possible explanation for the higher hydrogenation selectivity observed for Pd.<sup>16</sup> A description of the possible ethylene hydrogenation mechanism on Pd(111) using cluster and periodic slab calculations was performed by Neurock and van Santen.<sup>17</sup> At low coverage surface the ethylene hydrogenation follows the Horiuti–Polanyi mechanism.<sup>5</sup> Other study of catalytic hydrogenation of the 1,3-butadiene on Pd(111) and Pt(111) was also reported.<sup>18</sup> On Pd(111), the formation of butane species is favored but on Pt(111) the formation of butane and butene species seems to be competitive. In case of the acetylene hydrogenation on Pd(111) surface, the reaction path was evaluated in two steps: ethylene and ethane formations.<sup>19</sup>

The main goal of this work is to study from a theoretical point of view the hydrogenation and isomerization reactions of monoolefins on a Pd surface. Specifically, we are interested on the relative relevance of the hydrogenation versus the isomerization

Horiuti–Polanyi mechanisms for *cis*-2-butene and *trans*-2-butene on a Pd(111).

## 2. Computational Details

A density functional theory (DFT) method that combines the plane-wave expansion of electronic orbitals and soft pseudopotentials (DACAPO code<sup>a</sup>) was used to compute the energy of the system in the different steps of hydrogenation mechanisms. The generalized gradient approximation (GGA) was used with the functional of Perdew and Wang.<sup>20,21</sup> The 2D Brillouin integrations were performed on a  $3 \times 3 \times 1$  Monkhorst–Pack grid. The fixed convergence of the plane-wave expansion was obtained with a cut-off of 500 eV. This value is based on our previous tests, which showed that the converged calculation error was lower than 0.01 eV. The olefin/Pd system was studied by representing the metallic surface with a perfect smooth surface, namely the Pd(111) face since this surface was one of the most experimentally studied for the hydrocarbon conversion reaction.<sup>13,22</sup> The Pd(111) surface was modeled with a slab containing three atomic metal layers with nine Pd atoms in each layer. In previous calculations, the effect of the numbers of metal layers was examined.<sup>17,23</sup> Three layers of Pd provide computationally efficient results. The Pd–Pd interatomic distance for the three layers was 2.751 Å, as the bulk experimental value.<sup>24</sup> No relaxation of the first metallic layer was considered because earlier works showed minimal effects for olefins adsorbed on Pd.<sup>25</sup> A three-dimensional periodic cell was constructed including a vacuum gap of  $\sim 16$  Å in the perpendicular direction to the metallic surface. The adsorption of different species was evaluated. In order to minimize the interaction between adsorbates in the hydrogenation–isomerization reactions, a  $(3 \times 3)$  unit cell was selected. The adsorbate species were placed in one side of the slab and were allowed to optimize completely their geometry.

In the case of free 2-butene isomers the geometry is planar, having internal angles of 120°. The C=C and C–C bond distances for both geometrical isomers are almost the same, in agreement with the previous theoretical study<sup>15</sup> (1.36, 1.53 Å for *cis*-2-butene and 1.34, 1.53 Å for *trans*-2-butene, respectively).

<sup>a</sup>DACAPO is a free software developed at the Center for Atomic-scale Materials Physics (CAMPS) funded by the Danish research council.

The reaction energy ( $E_{\text{react}}$ ) between a  $\text{C}_4\text{H}_y$  moiety and  $x$  hydrogen atoms is defined as

$$E_{\text{react}} = E_{\text{C}_4\text{H}_y/\text{sup}} + xE_{\text{H}_{\text{ads}}/\text{sup}} - (1+x)E_{\text{sup}} - E_{\text{C}_4\text{H}_8(\text{g})} - E_{\text{H}_2(\text{g})} \quad (1)$$

where  $E_{\text{C}_4\text{H}_y/\text{sup}}$  is the energy of the adsorbed  $\text{C}_4\text{H}_y$  moiety,  $E_{\text{H}_{\text{ads}}/\text{sup}}$  the energy of the adsorbed H atom,  $E_{\text{sup}}$  the Pd surface energy,  $E_{\text{C}_4\text{H}_8(\text{g})}$  is the energy of the 2-butene isomers in gas phase, and  $E_{\text{H}_2(\text{g})}$  is the energy of the  $\text{H}_2$  molecule also in gas phase; moreover,  $x$  is the number of hydrogen atoms adsorbed on the Pd surface ( $x = 0 - 2$ ) and  $y = 8 - x$ . The reference value for the energy profiles is that corresponding to 2-butenes and two H adsorbed atoms at infinite distance. On the other hand, the adsorption energies ( $E_{\text{ads}}$ ) of an adsorbate were calculated by subtracting the energy of the gas-phase adsorbate plus the energy of the bare metal surface from the energy of the adsorbate-metal system:

$$E_{\text{ads}} = E_{\text{adsorbate}/\text{metal}} - E_{\text{adsorbate}} - E_{\text{metal}} \quad (2)$$

The evolution of molecular structure between intermediate states was evaluated by changing the interatomic distance between atoms A and B, considering equal spaced intervals. For each step of A-B breaking, the other geometrical parameters were optimized, except the C-H bond distance. In this way, a local maximum in PES surface can be obtained, enabling us to define a molecular structure whose energy gives a measure of the amount of energy required to activate the molecule from one intermediate state to the other. For a better

definition of the local maximum position smaller intervals were used.

### 3. Results and Discussion

#### 3.1. Intermediate species

Horiuti-Polanyi mechanism is the most accepted mechanism for the hydrogenation reactions of unsaturated hydrocarbons chains on transition metal catalysts. In case of monoolefins it comprises the opening of C=C double bond and the formation of an alkyl by inserting a coadsorbed hydrogen atom into the unsaturated adsorbed molecule. The subsequent addition of another hydrogen atom to the half-hydrogenated intermediate yields the corresponding alkane, which easily desorbs from the catalytic surface.

Before performing an analysis of the whole hydrogenation mechanism of *cis/trans*-2-butene, the adsorption of these molecules and their respective alkyls were considered. From the previous published results for the adsorption of ethylene on Pd,<sup>26</sup> it appears that the di- $\sigma$  configuration has the more relevant chemical interaction with the metallic surface in comparison with the  $\pi$  configuration. For this reason, the di- $\sigma$  adsorption for *cis/trans*-2-butene is considered in the present work. This assumption is also supported by the interpretation of high-resolution IR spectra obtained for ethylene hydrogenation on Pt.<sup>27</sup>

In Table 1, the values of  $E_{\text{react}}$  and geometric molecular parameters for adsorbed *cis/trans*-2-butene and 2-butyl isomers are summarized.

Table 1. Reaction energies ( $E_{\text{react}}$ , kcal/mol) and more relevant geometrical parameters (distances in Å, angles in degrees) of the reactants and the intermediate species for the hydrogenation and isomerization mechanisms on Pd(111) surface.

Adsorbate	$E_{\text{react}}$	$d(\text{Pd}-\text{C})$	$d(\text{C}-\text{C})$	$d(\text{H}-\text{Pd})$	$\angle(\text{C}-\text{Pd}_1-\text{Pd}_2)$	$\angle(\text{C}-\text{C}-\text{Pd}_1)$
<i>cis</i> -2-Butene	-32.2 (-25.1) <sup>a</sup>	2.20	1.48		73.2	106.8 (18.0) <sup>b</sup>
<i>trans</i> -2-Butene	-29.3 (-23.0) <sup>a</sup>	2.20	1.45		72.8	107.2 (29.0) <sup>b</sup>
<i>eclipsed</i> -2-Butyl	-17.9	2.16	1.62	2.01	91.3	111.3
<i>staggered</i> -2-Butyl	-24.1	2.16	1.55	2.02	90.5	112.4
<i>eclipsed</i> -2-Butyl + H <sup>c</sup>	-8.0	2.28	1.62	1.93	85.4	113.3
<i>staggered</i> -2-Butyl + H <sup>c</sup>	-18.9	2.29	1.55	1.94	85.2	113.6

<sup>a</sup>Between parentheses, the  $E_{\text{react}}$  values for coadsorption with a neighboring H atom.

<sup>b</sup>Between parentheses, the  $\theta$  angle shown in Fig. 2.

<sup>c</sup>For coadsorption with a neighboring H atom.

The calculated adsorption energies for *cis*-2-butene and *trans*-2-butene are  $-10.03$  and  $-7.06$  kcal/mol, respectively. These values are in agreement with the results obtained by Lee and Zaera<sup>28</sup> for 2-butene adsorbed on Pt(111). Indeed, the reported TPD spectra showed a desorption peak at 230 K due to *cis*-2-butene and another peak at 200 K due to *trans*-2-butene, associated to desorption energies of 13.4 and 11.6 kcal/mol, respectively. On the other hand, recent theoretical DFT calculations for 2-butene on Pt(111) and Pd(111) obtained also the same trend for Pt, but the magnitude of adsorption energies is somewhat greater ( $\approx 6$  kcal/mol) than the experimental desorption energies.<sup>15</sup> In case of Pd(111), the adsorption energies are greater than our results ( $\approx 5$  kcal/mol).

Regarding the geometrical parameters of *cis*/*trans*-2-butene isomers, we notice that their geometries are modified with respect to the free molecules. For both the isomers, the C<sub>2</sub>-C<sub>3</sub> bond is parallel to the surface (see Figs. 1(a) and 1(b)) and undergoes an elongation with respect to the *cis*/*trans*-2-butene free species (1.48–1.45 Å versus 1.36–1.34 Å, respectively). This stretching is slightly higher for *cis*-2-butene, a result that follows the same trend as

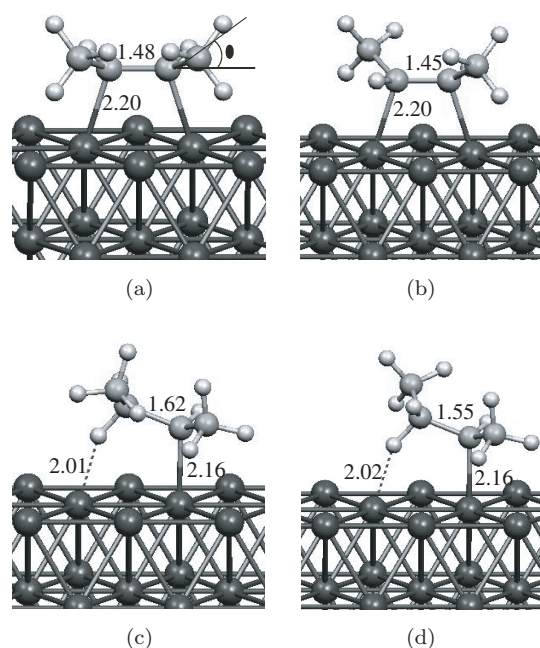


Fig. 1. 2-Butene reactants and 2-butyl intermediates adsorbed on Pd(111): (a) *cis*-2-butene, (b) *trans*-2-butene, (c) *eclipsed*-2-butyl, and (d) *staggered*-2-butyl.

revealed by X-ray absorption spectroscopy data.<sup>29</sup> The C<sub>2</sub> and C<sub>3</sub> atoms adopt the sp<sup>3</sup> hybridization, proved by the H-C-C-CH<sub>3</sub> torsion angle which changes from 180°, for the gas phase, to 134° for the adsorbed species. This modification is higher than that obtained for the ethylene molecule (from 180° to 143°, Ref. 17), mainly due to the methyl groups. The deformation of the molecule upon adsorption is also evident because the  $\beta$  methyl groups point outwards the metal surface, the molecule losing its original planarity (see angle  $\theta$  in Figs. 1(a) and 1(b)). The calculated C<sub>2</sub>-C<sub>3</sub> and C-Pd interatomic distances are very similar to the theoretical values reported previously for ethylene and 2-butene on Pd.<sup>15,17</sup> Particularly, our C<sub>2</sub>-C<sub>3</sub> distances for *cis*/*trans*-2-butene differ by  $+0.02/-0.01$  Å and the C-Pd distance by  $+0.05/+0.06$  with the data reported by Valcárcel *et al.*<sup>15</sup>

The half-hydrogenated intermediates produced from *cis* and *trans*-2-butene are the *eclipsed* and *staggered*-2-butyl isomers, respectively. These adsorbed alkyls are less stable than the corresponding 2-butene reactants. Looking the  $E_{\text{react}}$  values at Table 1, we observe that the effect is more noticeable for the *eclipsed* than for the *staggered* isomer (14.3 and 5.2 kcal/mol, respectively). Both radicals adsorb in an on-top configuration, forming a C-Pd<sub>1</sub>-Pd<sub>2</sub> angle of 91.3° and 90.5° for *eclipsed* and *staggered*-2-butyl, respectively (see Figs. 1(c)–1(d) and Table 1). Two different interactions are formed with the solid: a Pd-C bond and a less significant C-H-Pd interaction mediated by the hydrogen of  $\beta$ -carbon. The Pd-C distances shorten slightly with respect to those of adsorbed 2-butene isomers and the C-H bond is relatively long due to the interaction with the surface Pd atom (1.13 Å). In general, the internal geometrical parameters are very similar for both radicals, excepting the C<sub>2</sub>-C<sub>3</sub> distance which is nearly 0.1 Å longer for the *eclipsed*-2-butyl. This distance takes a value very similar to that of free butane (1.56 Å).

### 3.2. Horiuti–Polanyi hydrogenation mechanism

In Figs. 2 and 3, the  $E_{\text{react}}$  profiles for the hydrogenation mechanism of *cis* and *trans*-2-butene, respectively, are shown. The geometries for activated states are shown in Figs. 4(a)–4(d). The respective  $E_{\text{react}}$

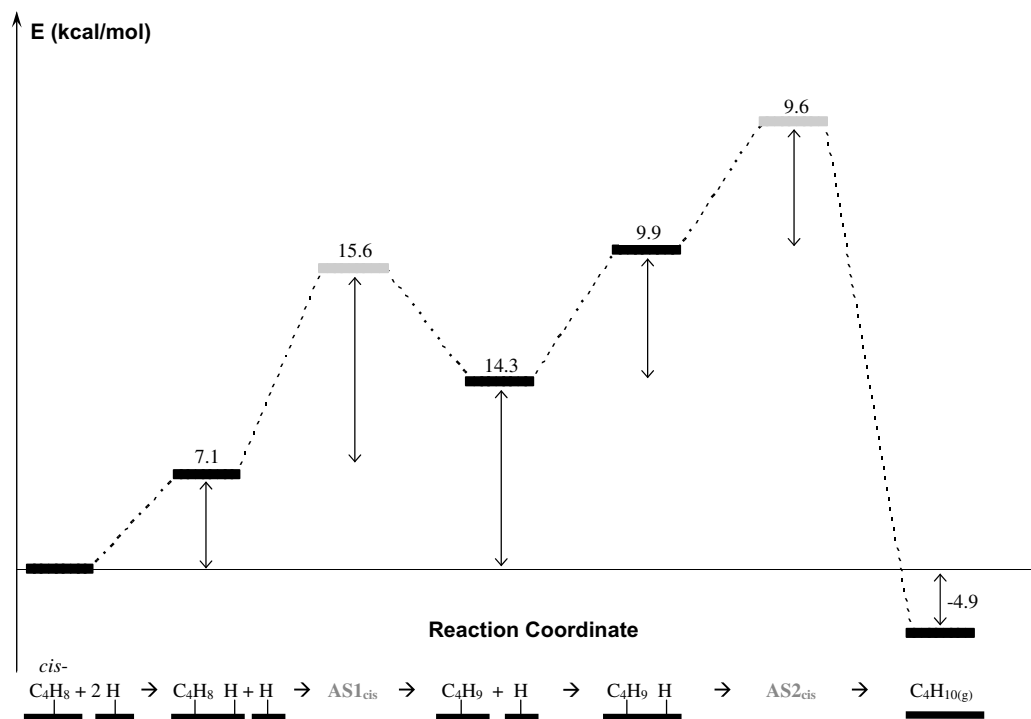


Fig. 2. Reaction energy profile of *cis*-2-butene hydrogenation on Pd(111) following the Horiuti–Polanyi mechanism. The grey steps correspond to activation barrier. The zero level corresponds to the adsorbed reactants infinitely separated.

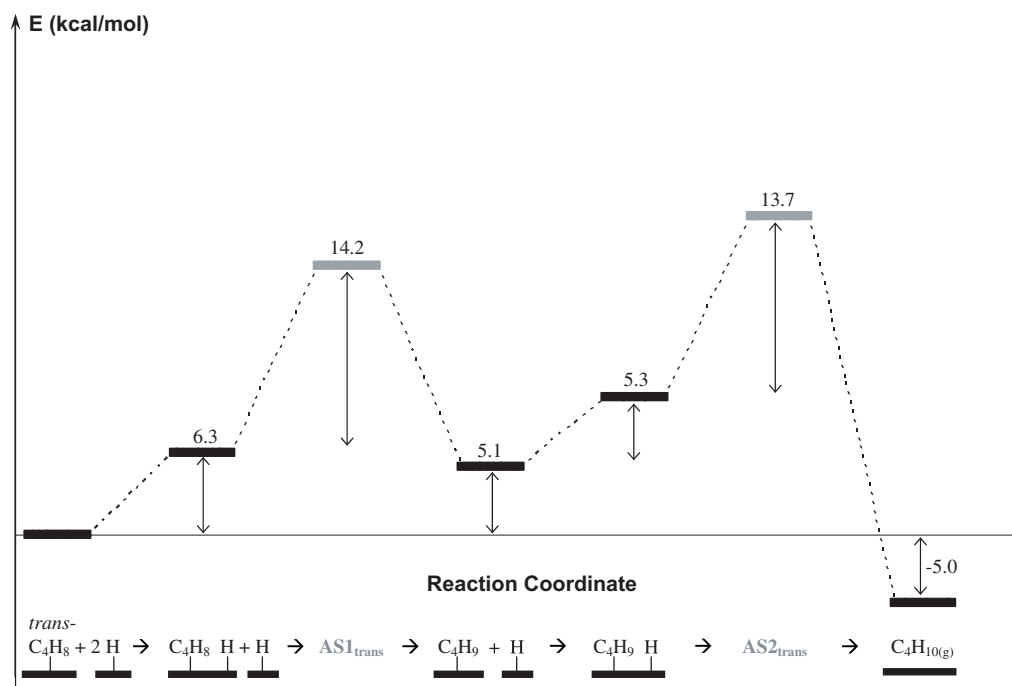


Fig. 3. Reaction energy profile of *trans*-2-butene hydrogenation on Pd(111) following the Horiuti–Polanyi mechanism. The grey steps correspond to the activation barriers. The zero level corresponds to the adsorbed reactants infinitely separated.

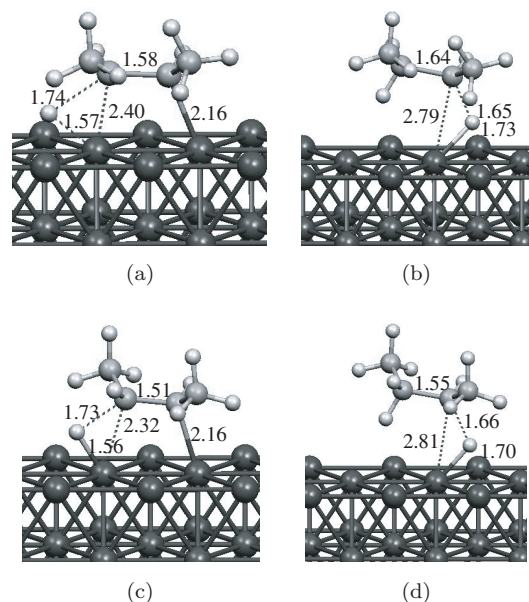


Fig. 4. Activated states for 2-butenes hydrogenation on Pd(111). For *cis*-2-butene hydrogenation: (a) AS1<sub>*cis*</sub>, (b) AS2<sub>*cis*</sub>. For *trans*-2-butene hydrogenation: (c) AS1<sub>*trans*</sub>, (d) AS2<sub>*trans*</sub>.

Table 2. Reaction energies ( $E_{\text{react}}$ , kcal/mol) and more relevant geometrical parameters (distances in Å, angles in degrees) for the activated intermediates in hydrogenation and isomerization mechanisms on Pd(111) surface.

Activated state	$E_{\text{react}}^{\text{a}}$	$d(\text{Pd}-\text{C})$	$d(\text{C}-\text{C})$	$d(\text{H}-\text{Pd})$	$d(\text{C}-\text{H})$
AS1 <sub><i>cis</i></sub>	-9.5 (22.7)	2.40	1.58	1.57	1.74
AS2 <sub><i>cis</i></sub>	+1.6 (33.8)	2.79	1.64	1.73	1.65
AS1 <sub><i>trans</i></sub>	-8.8 (20.5)	2.32	1.51	1.56	1.73
AS2 <sub><i>trans</i></sub>	-5.2 (24.1)	2.81	1.55	1.70	1.66
AS2 <sub><i>isom</i></sub>	-15.3 (16.9)	2.14	1.64	2.11	1.12

<sup>a</sup>Between parentheses, the  $E_{\text{react}}$  values referred to the initial state of the reaction path.

and more relevant geometrical parameters are summarized in Table 2.

Starting with an adsorbed 2-butene molecule and an adsorbed H atom infinitely separated on the Pd surface, one H atom is placed on a threefold fcc hollow site close to the C<sub>2</sub> atom of adsorbed

butane. The interaction with the H atom produces a destabilization of  $\sim 6.5$  kcal/mol of 2-butene isomers, with no significant change in their geometries (see Table 1). This observation is in agreement with recent TPD results for 2-butene adsorbed on a H<sub>2</sub>-predosed Pt(111) surface, which reveal a significant shift in desorption peaks to lower temperatures.<sup>10</sup> Similar theoretical results have been reported for butadiene adsorbed on Pt and Pd.<sup>18</sup> Afterwards, the coadsorbates react to produce the *eclipsed* and *staggered*-butyl intermediates, coming from *cis* and *trans*-2-butene, respectively. This first H atom addition comprises the rupture of Pd-C<sub>2</sub> and Pd-H bonds and the creation of C<sub>2</sub>-H bond. The geometry of the corresponding activated state (AS1<sub>*cis*</sub> and AS1<sub>*trans*</sub> for *cis* and *trans*-2-butene, respectively) shows a three-center C-H-Pd interaction, with the H atom more strongly linked to the Pd of original Pd-C<sub>2</sub> bond than to the C<sub>2</sub> atom of isomer (see Figs. 4(a) and 4(c) and Table 2). The Pd-H bond can be viewed as the nascent C-H-Pd interaction of 2-butyl intermediate (see Sec. 3.1). The energy barrier for the first H addition on *cis*-2-butene is 15.6 kcal/mol and on *trans*-2-butene 14.2 kcal/mol, making the AS1<sub>*cis*</sub> state less stable than the AS1<sub>*trans*</sub> state. The energy balance for the production of intermediate radicals is endothermic (7.2 kcal/mol) for *cis*-2-butene and exothermic (1.2 kcal/mol) for *trans*-2-butene.

The second H atom addition entails the interaction of another H atom adsorbed on the threefold fcc hollow site close to the C<sub>3</sub> atom of adsorbed 2-butyl. This interaction is repulsive, giving an energy destabilization (9.9 and 5.3 kcal/mol, for *eclipsed* and *staggered*-2-butyl, respectively). Furthermore, this interaction is accompanied by a modification in adsorbed alkyl geometry: a significant elongation of Pd-C bond and a marked decrease in C-Pd<sub>1</sub>-Pd<sub>2</sub> angle can be observed (see Table 1). The reaction of H and alkyl coadsorbates gives the butane molecule in gas phase and the bare metallic surface. The corresponding activated state (AS2<sub>*cis*</sub> and AS2<sub>*trans*</sub> for *eclipsed* and *staggered*-2-butyl, respectively) implies a three-center C-H-Pd interaction as in the first H atom addition. Nevertheless, these activated states are less stable than the AS1<sub>*cis*</sub> and AS1<sub>*trans*</sub> states (11.1 and 3.6 kcal/mol, respectively). Moreover, the Pd-C and Pd-H interatomic distances for AS2 activated states are larger than those for AS1 ones (0.4-0.5 Å and 0.15 Å, respectively),

as it can be observed in Figs. 4(b) and 4(d) and in Table 2. The hydrogenation energy barrier for *eclipsed*-2-butyl is 9.6 kcal/mol and for *staggered*-2-butyl 13.7 kcal/mol. The energy balance for the final production of butane and bare Pd surface is exothermic for both the *eclipsed*-2-butyl and *staggered*-2-butyl (29.1 and 15.4 kcal/mol, respectively).

Regarding the whole hydrogenation for the 2-butenes isomers, we notice that they are exothermic (nearly 5 kcal/mol). The intermediate states produced during the *cis*-2-butene hydrogenation are in general less stable than those of the *trans*-2-butene hydrogenation. Moreover, the energy barrier for whole *cis*-2-butene hydrogenation is higher (9.7 kcal/mol) than that for whole *trans*-2-butene hydrogenation. It is noteworthy that in both cases the energy barrier for the first H atom addition is larger than that for the second (15.6/9.6 and 14.2/13.7 kcal/mol for *cis* and *trans*-2-butene,

respectively). This observation is in agreement with the experimental evidence for ethylene and propylene hydrogenation on Pt, arguing an initial half-hydrogenation slow step.<sup>6,7</sup> Analogous theoretical results have been obtained for the hydrogenation of ethylene on Pd.<sup>17</sup>

In order to rationalize the different behaviors of 2-butene isomers during their hydrogenation on Pd(111), the densities of electronic states projected (PDOS) on selected atomic orbitals of the adsorbate/surface system were calculated. Looking at the geometries in Figs. 4(a) and 4(c), we observe that the most relevant link between the  $AS1_{cis}$  and  $AS1_{trans}$  activated states and the Pd surface is the C<sub>2</sub>-Pd bond. The atomic orbitals with the appropriate symmetry along the axis of this bond are the p<sub>z</sub> orbital of the C<sub>2</sub> atom and the d<sub>z</sub><sup>2</sup> orbital of nearest surface Pd atom. Figure 5(a) shows the PDOS of C<sub>2</sub>(p<sub>z</sub>) and Pd(d<sub>z</sub><sup>2</sup>) orbitals for the  $AS1_{cis}$ /Pd system and

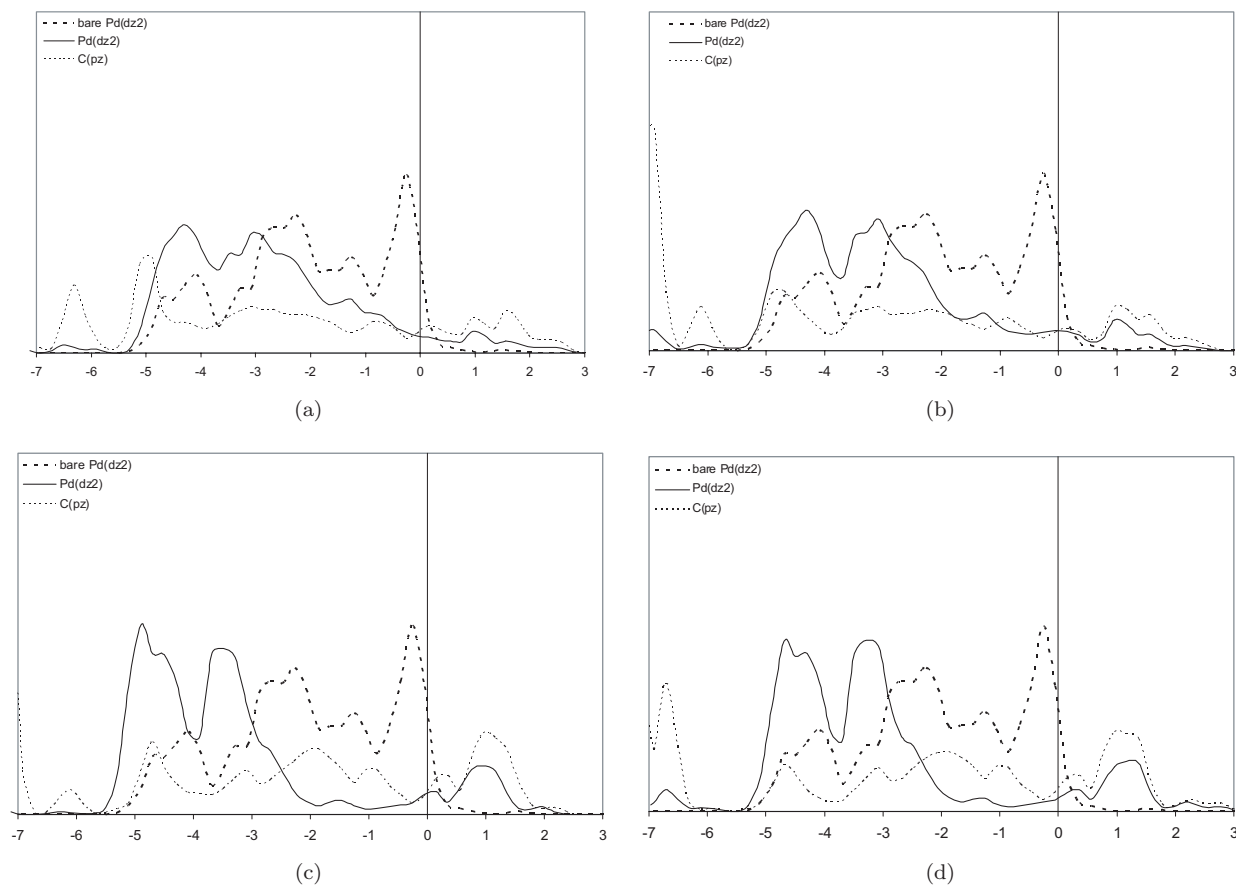


Fig. 5. Projected density of states (PDOS) onto C<sub>2</sub>(p<sub>z</sub>) and Pd(d<sub>z</sub><sup>2</sup>) atomic orbitals: (a)  $TS1_{cis}$ , (b)  $TS1_{trans}$ , (c) *eclipsed*-2-butyl, and (d) *eclipsed*-2-butyl on Pd(111). Energies are expressed in eV and PDOS in au.

Fig. 5(b) for the  $AS1_{trans}/Pd$  system. For comparison, the PDOS of  $d_z^2$  orbital for the clean Pd surface was also included. It is noteworthy the modifications undertaken by the  $d_z^2$  band due to the interaction between  $AS1_{cis}$  and Pd surface, in comparison with the bare surface. This band broadens exhibiting a significant decrease in the number of occupied states near the Fermi level, an enlargement of PDOS at the bottom of the band and the appearance of new states above the Fermi level. This observation can be related to the presence of an important coupling between the  $C_2(d_z^2)$  and  $Pd(p_z)$  orbitals, by comparison of respective PDOS profiles. This  $d_z^2$  band broadening is more noticeable in the case of  $AS1_{trans}/Pd$ , implying a stronger interaction than that obtained in the  $AS1_{cis}/Pd$  system. The last observation is in agreement with the relative stability of these activated states, as commented above.

Figures 5(c) and 5(d) show the PDOS of  $C_2(p_z)$  and  $Pd(d_z^2)$  orbitals for the *eclipsed*-2-butyl/Pd and *staggered*-2-butyl/Pd systems. The electronic structure of these systems reveals the same general properties as those observed in the previous activated state: a  $d_z^2$  band broadening and an important

coupling of these atomic orbitals. The  $d_z^2$  band broadening is more noticeably in the case of *staggered*-2-butyl/Pd system, in agreement with the greater stability obtained for the latter intermediate.

### 3.3. Horiuti-Polanyi isomerization mechanism

In the hydrogenation process of olefins, the hydrogenation and isomerization reactions elapse simultaneously. In the case of 2-butenes, the isomerization implies the production of *trans*-2-butene from *cis*-2-butene or, vice-versa, that of *cis*-2-butene from *trans*-2-butene. The formation of 1-butene could be another alternative, but it has not been reported for transition metal catalysts.<sup>14</sup> Within the Horiuti-Polanyi mechanism, the same half-hydrogenated intermediate (alkyl) is present for both reactions. After the conversion of one 2-butyl isomer to the other stereospecific radical, a later dehydrogenation gives the corresponding unsaturated hydrocarbon isomer.

In Fig. 6, the  $E_{react}$  profile for the isomerization mechanism of *cis*-2-butene is shown. The geometries

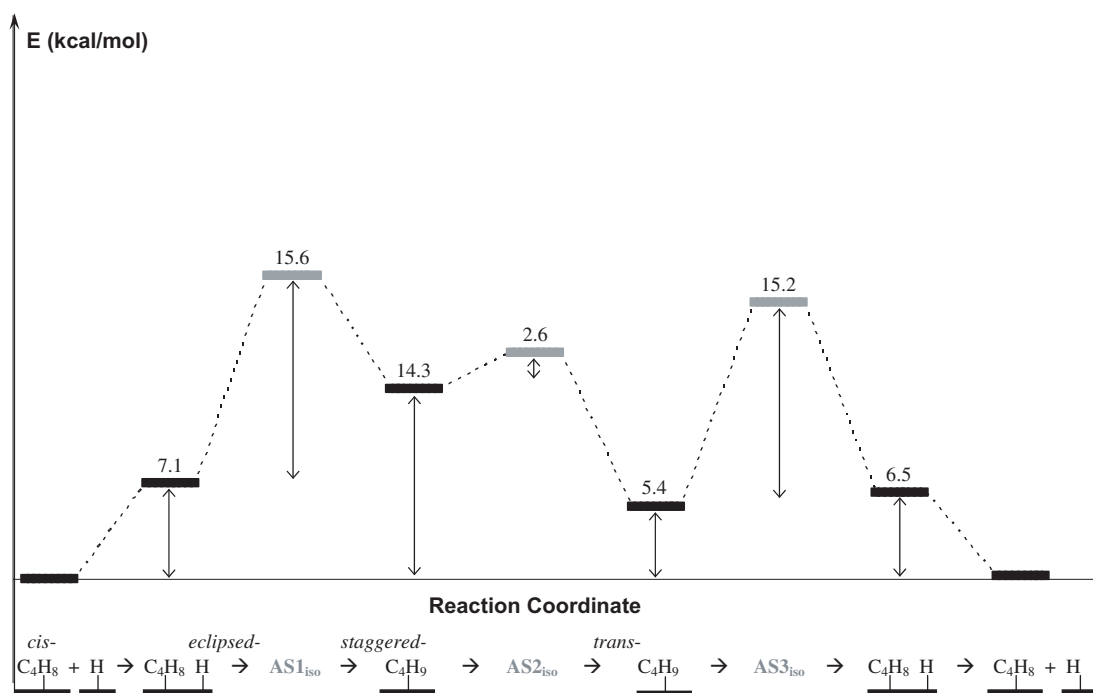


Fig. 6. Reaction energy profile of 2-butene isomerization on Pd(111) following the Horiuti-Polanyi mechanism. The grey steps correspond to the activation barriers. The zero level corresponds to the adsorbed reactants infinitely separated.



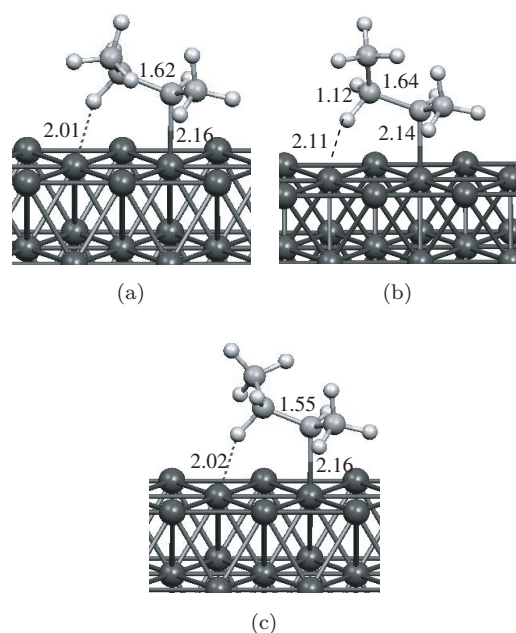


Fig. 7. Activated states for 2-butene isomerization on Pd(111). (a) AS1<sub>iso</sub>, (b) AS2<sub>iso</sub>, and (c) AS3<sub>iso</sub>.

for activated states are shown in Figs. 7(a)–7(c). The respective  $E_{\text{react}}$  and more relevant geometrical parameters are summarized in Table 2. In order to compare the  $E_{\text{react}}$  profiles of the isomerization mechanism with that of the hydrogenation mechanism an extra hydrogen atom had to be included in the evaluation of  $E_{\text{react}}$  values.

The mechanism starts from an adsorbed *cis*-2-butene molecule and an adsorbed H atom infinitely

separated on the Pd surface. The following two steps of the isomerization are equivalent to those of the first H atom addition. The produced half-hydrogenated intermediate, the *eclipsed*-2-butyl radical, presents an easy rotation of the  $\beta$ -carbon with  $sp^3$  hybridization, giving a subsequent intermediate, the *staggered*-2-butyl isomer. The geometry of the corresponding activated state AS2<sub>iso</sub> shows a substantially larger distance between the H of  $\beta$  carbon atom C<sub>2</sub> and the nearest Pd atom of the surface in comparison with the adsorbed 2-butyl isomers (2.11 Å versus 2.01–2.02 Å). The energy barrier for converting the *eclipsed*-2-butyl into the *staggered*-2-butyl is 2.6 kcal/mol. The later two steps of the isomerization mechanism are equivalent to the two initial steps in the *trans*-2-butene hydrogenation, but performed in the opposite sense. The last step of the isomerization mechanism finishes with the adsorbed *trans*-2-butene and the hydrogen atom are infinitely separated.

Figure 8 shows the PDOS of C<sub>2</sub>(p<sub>z</sub>) and the Pd(d<sub>z<sup>2</sup></sub>) orbitals for the AS2<sub>iso</sub>/Pd system. The electronic structure of this system reveals greater d<sub>z<sup>2</sup></sub> band broadening and coupling of these atomic orbitals than those observed for the AS1<sub>cis</sub>/Pd and AS1<sub>trans</sub>/Pd systems. This result is in agreement with the greater stability obtained for the AS2<sub>iso</sub> activated state.

The isomerization reaction for the *cis*-2-butene is slightly endothermic (0.2 kcal/mol) and the production of *trans*-2-butene can be considered

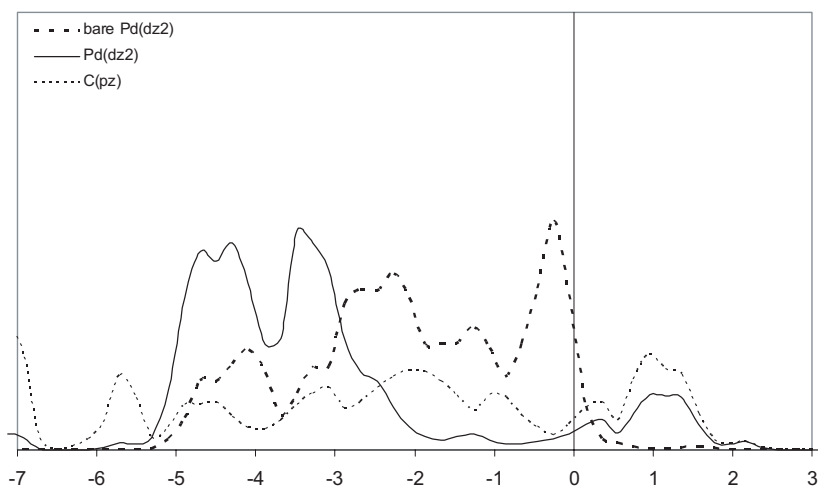


Fig. 8. Projected density of states (PDOS) onto C2(p<sub>z</sub>) and Pd(d<sub>z<sup>2</sup></sub>) atomic orbitals: AS2<sub>iso</sub> on Pd(111). Energies are expressed in eV and PDOS in au.

as thermodynamically equilibrated. Nevertheless, comparing the  $E_{\text{react}}$  values for 2-butene molecules in interaction with a neighboring H atom, a 0.6 kcal/mol energy gain is obtained. From this, we infer that the isomerization from *cis*-2-butene to *trans*-2-butene can be considered as a thermodynamically feasible process. Moreover, the energy required to activate the *eclipsed*-2-butyl intermediate (2.6 kcal/mol), across the AS<sub>2iso</sub> state, is much lower than that to activate the *staggered*-2-butyl (11.5 kcal/mol), making easier the path for producing *trans*-2-butene.

Once the *eclipsed*-2-butyl intermediate is produced, we have two competitive reactions: the above discussed isomerization or a second H atom addition. The former continues by the easy production of *staggered*-2-butyl. At this stage, the energy barrier required to complete the isomerization is 15.2 kcal/mol. On the other hand, the energy for the direct addition of a second H atom to the *eclipsed*-2-butyl intermediate is 19.5 kcal/mol. As a consequence, the isomerization would be the fastest reaction. However, in actual working conditions of catalysts, the presence of H atoms in the neighborhood of *eclipsed*-2-butyl (for example, due to higher pressures) must push up its  $E_{\text{react}}$ , reducing the barrier for the second H addition to 9.6 kcal/mol. In these conditions a fast hydrogenation reaction would be expected. Another alternative is a second H atom addition mediated through the *staggered*-2-butyl. In this case, the energy barrier required for the completion the hydrogenation is 19.0 kcal/mol.

#### 4. Conclusions

The Horiuti–Polanyi mechanisms for 2-butene hydrogenation and isomerization on Pd(111) were studied by using periodic DFT calculations. The hydrogenations of *cis* and *trans*-2-butene comprise the sequential addition of two hydrogen atoms and a half-hydrogenated intermediate. The alkyl intermediate for *cis*-2-butene hydrogenation (the *eclipsed*-2-butyl) is less stable than that for *trans*-2-butene hydrogenation (the *staggered*-2-butyl). In both cases, a relatively high energy barrier to produce the half-hydrogenated intermediate makes the first hydrogen addition the slowest step of the reaction. The isomerization of *cis*-2-butene to give *trans*-2-butene comprises the conversion from *eclipsed* to

*staggered*-2-butyl intermediates. The activated state between them is much stable than the other activated states of the reaction path. Our results indicate that the energy barrier for isomerization would depend markedly on the hydrogen coverage.

#### Acknowledgments

The authors thank the financial support from the Consejo Nacional de Investigaciones Científicas y Técnicas (CONICET), the Agencia de Promoción Científica y Tecnológica (Project PICT2003-14-14582), and the Universidad Nacional del Sur (UNS).

#### References

1. G. C. Bond, *Metal-Catalyzed Reactions of Hydrocarbons* (Springer, New York, 2005).
2. J. M. Brown, *Angew. Chem. Int. Ed.* **26** (1987) 190.
3. M. Plourde, K. Belkacemi and J. Arul, *Ind. Eng. Chem. Res.* **43** (2004) 2382.
4. C. Godínez, A. L. Cabanes and G. Villora, *Chem. Eng. Proc.* **34**(5) (1995) 459.
5. J. Horiuti and M. Polanyi, *Trans. Faraday Soc.* **30** (1934) 1164.
6. F. Zaera, *Langmuir* **12** (1996) 88.
7. F. Zaera and D. Chrysostomou, *Surf. Sci.* **457** (2000) 89.
8. Z. Ma and F. Zaera, *Surf. Sci. Rep.* **61** (2006) 229.
9. F. A. Kummerow, Q. Zhou and M. M. Mahfouz, *Am. J. Clin. Nutri.* **70** (1999) 832.
10. I. Le and F. Zaera, *J. Phys. Chem. B* **109** (2005) 2745.
11. I. Le and F. Zaera, *J. Phys. Chem. C* **111** (2007) 10062.
12. C. Yoon, M. X. Yang and G. A. Somorjai, *Catal. Lett.* **46** (1997) 37.
13. G. Tourillon, A. Cassuto, Y. Jugnet, J. Massadier and J. C. Bertolini, *J. Chem. Soc. Faraday Trans.* **92** (1996) 4835.
14. C. Yoon, M. X. Yang and G. Somorjai, *J. Catal.* **176** (1998) 35.
15. A. Valcárcel, A. Clotet, J. M. Ricat, F. Delbecq and P. Sautet, *Surf. Sci.* **549** (2004) 121.
16. F. Mittendorfer, C. Thomazeau, P. Raybaud and H. Toulhoat, *J. Phys. Chem. B* **107** (2003) 12287.
17. M. Neurock and R. A. van Santen, *J. Phys. Chem. B* **104** (2000) 11127.
18. A. Valcárcel, A. Clotet, J. M. Ricat, F. Delbecq and P. Sautet, *J. Phys. Chem. B* **109** (2005) 14175.
19. D. Mei, P. A. Sheth, M. Neurock and C. M. Smith, *J. Catal.* **242** (2006) 1.
20. J. P. Perdew and Y. Wang, *Phys. Rev. B.* **33** (1986) 8800.
21. J. P. Perdew and Y. Wang, *Phys. Rev. B.* **45** (1992) 13244.

22. J. C. Bertolini, A. Cassuto, Y. Jugnet, J. Massadier, B. Tardy and G. Tourillon, *Surf. Sci.* **349** (1996) 88.
23. P. Venkataraman, M. Neurok, L. B. Hansen, B. Hammer and J. K. Norskov, *Phys. Rev. B* **60** (1999) 6146.
24. R. W. G. Wyckoff, *Crystal Structures*, 2nd edn. Vol. 1 (Interscience, New York, 1965).
25. M. Neurock and R. A. van Santen, *J. Phys. Chem. B* **104** (2000) 11132.
26. Q. Ge and M. Neurock, *Chem. Phys. Lett.* **358** (2002) 377.
27. P. S. Cremer, X. Su, Y. R. Shen and G. A. Somorjai, *J. Am. Chem. Soc.* **118** (1996) 2942.
28. I. Lee and F. Zaera, *J. Am. Chem. Soc. Commun.* **127** (2005) 12174.
29. A. Cassuto and G. Tourillon, *Surf. Sci.* **309** (1994) 65.

